Formation of disordered structures in Cr-Fe alloy by mechanical milling

Formation of disordered structures in Cr–Fe alloy by mechanical milling

S K Xia[†], E Baggio-Saitovitch[†], F C Rizzo Assunção[‡] and V A Peña Rodríguez[†]

† Centro Brasileiro de Pesquisas Fisicas, Rua Xavier Sigaud 150, 22290 Rio de Janeiro, Brazil
‡ Departamento Ciência dos Materiais e Metalurgia, Pontificia Universidade Catolica do Rio de Janeiro, 38008 Rio de Janeiro, Brazil

Abstract. Mechanical milling was performed on the alloy $Cr_{72}Fe_{28}$. X-ray diffraction and Mössbauer spectroscopy were used to follow the progress of the structural variation. The experimental results can be interpreted by assuming that the milled powders are composed of a small amount of crystalline component and two disordered components: one with a random densely packed structure and the other with a random loosely packed structure. Moreover, differential scanning calorimetry was used to obtain the crystallization temperature. A mechanism was proposed to describe the formation of the disordered structures as well as the structural stability in this alloy.

1. Introduction

Conventionally, the ratio of the atomic radii between the two constituents of a binary alloy is considered to be an important criterion in evaluating the glass-forming ability (Giessen 1982, Davies 1983). The difference between the atomic radii generally should be larger than about 15%. Therefore, for many binary alloys an amorphous phase cannot be achieved by rapid quenching from the melt. One of these systems is Cr–Fe in which the two constituents have similar atomic sizes (the bond lengths for Cr and Fe in the BCC structure are 0.249 80 nm and 0.248 23 nm respectively (Weast 1965–6)). However, it is conceivable that, if the long periodical structure is destroyed at a temperature lower than the crystallization temperature and if subsequent relaxation towards a crystalline structure does not occur, the resulting amorphous structure may be retained. Recently, Kuwano *et al* (1992) proposed that a mechanical milled Cr–Fe alloy powder was composed of nanosized crystallities and grain boundaries, which were comparable with the nanocrystalline materials obtained using an inert gas condensation technique (Birringer *et al* 1984). In a preliminary work (Rodríguez *et al* 1992), we reported the alloying of Cr and Fe elemental powders by a mechanical alloying process. In this investigation, we shall report the mechanical milling (MM) of a Cr–Fe alloy and propose that, by long-time ball milling of the alloy $Cr_{72}Fe_{28}$, a disordered structure can be formed.

As is well known, during milling, an amount of free energy can be stored in the material because of cold working. As a consequence, amorphization may take place if the free energy of the system is higher than that of the amorphous phase (Schultz 1988). So far, two mechanisms of amorphous phase formation by ball milling have been proposed.

The first proposed that amorphization is caused by the fast interdiffusion between the two constituents with a large difference between their diffusivities and enthalpies of mixing and it is believed that the mechanical alloying of elemental powders belongs to this class (Koch *et al* 1983, Weeber *et al* 1986, Hellstern and Schultz 1987). The other proposal is that amorphization takes place through the accumulation of lattice defects such as vacancies, interstitials and dislocations, which can explain amorphization for intermetallic compounds with a narrow homogeneous range (Schwarz and Koch 1986, Weeber *et al* 1987). Schwarz and Koch (1986) suggested that, for intermetallic compounds with a narrow homogeneous range, amorphization may take place when there is a critical concentration of lattice defects above which the structure of the compound is unstable. Since the starting material studied in this investigation is a solid solution, modification of the latter mechanism is proposed in this work to explain the amorphization process.

2. Experimental details

The starting powder was prepared from a homogeneous $Cr_{72}Fe_{28}$ crystalline alloy arc melted in an argon atmosphere. To ensure further homogenization, the sample was annealed at 1173 K for 4 days and then quenched in water. The ball milling was performed in a vibration frame using a hardened steel vial and 16 balls, five with a diameter of 1.5 cm and 11 with a diameter of 1 cm. The sample was sealed in the vial filled with argon gas. Each time that part of the sample was collected for measurement, the vial was opened inside a glove-box filled with purified argon gas. During milling, the vial was kept at room temperature (RT).

The effect of MM on the structure of the milled powders was followed by x-ray diffraction using Cu Kα radiation performed on a Philips x-ray diffractometer equipped with an LiF monochromator.

The thermal stability was studied by differential scanning calorimetry (DSC) carried out on a TA 9900-DSC mod-951 system at a heating rate of 20 K min^{-1}.

Mössbauer spectra were measured at RT and 4.2 K in transmission geometry using a 30 mCi ^{57}Co source in an Rh matrix. The RT and 4.2 K spectra were fitted by a quadrupole splitting distribution (QSD) and a hyperfine field distribution (HFD), respectively, using the histogram method described by Brand and Le Caer (1988). To reproduce the asymmetry of the spectra, a linear correlation between the quadrupole splitting (QS) (or hyperfine field B_{hf}) and isomer shift (IS) was assumed.

The chemical compositions were determined by energy-dispersive analysis in an electron microprobe. The results for the starting powder and the powder milled for 200 h (called sample FC200 hereafter) are shown in table 1. The increase in the Fe content and the introduction of a small amount of Ni are due to contamination from the steel balls and the vial wall during milling. Although Cr has a high affinity for oxygen, no Cr oxide was detected within the limitation of x-ray diffraction for the as-milled powder and for the powder annealed in a vacuum of 5×10^{-6} Torr at 1173 K for 4 h. Similarly, no Fe oxide or Cr–Fe oxide were detected within the limitation of Mössbauer spectroscopy.

3. Experimental results

3.1. X-ray diffraction

Figure 1 shows the x-ray diffraction patterns of the starting powder, the milled powders and

Table 1. Chemical composition of powders as filled and milled for 200 h.

Sample	Amount (at.%)		
	Fe	Cr	Ni
As filled	28	72	0
Milled for 200 h	35	65	<0.4

the recrystallized powder sample FC200 after an anneal at 873 K for 2 h. Two features can be seen.

(a) With increasing milling time, the intensity of the maximum of the diffracted peak decreases and the width becomes broader. For sample FC200 only a single broad peak is observed.

(b) The most intense diffracted peak shifts from $2\theta = 44.6°$ for the starting powder to $43.8°$ for the powder sample FC200.

Figure 2 shows the milling time dependence of 'effective crystallite size' which can be taken as an ordering correlation length. This is estimated from the FWHM of line (110) of the x-ray diffraction pattern using the Scherrer formula $L = 0.91\lambda/(\beta \cos\theta)$, where λ is the x-ray wavelength, β the FWHM in radians and θ the position of the peak. After milling for 200 h, the value of L is about 1.5 nm. That is, at this stage the diffraction pattern appears to be that of an amorphous structure.
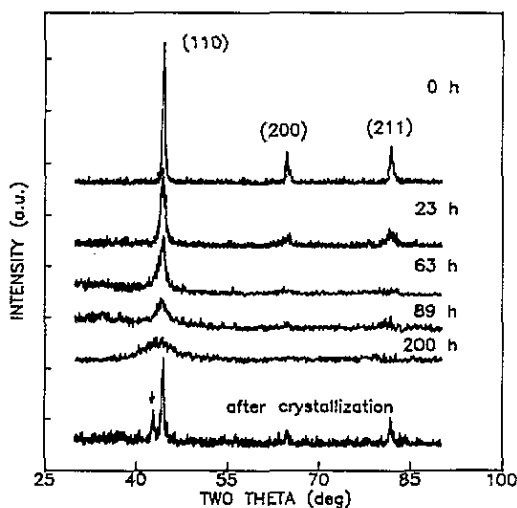

Figure 1. X-ray diffraction patterns of Cr–Fe starting powder, milled powders for the indicating milling times and recrystallized powder (a.u., arbitrary units).

For the recrystallized powder, besides the recovery of BCC Cr–Fe alloy phase, a precipitated phase can be seen (arrow). This precipitated phase, according to Saiki *et al* (1985), may be a Cr-rich phase.

3.2. Mössbauer spectroscopy

Figure 3 shows the Mössbauer spectra measured at 4.2 K for the Cr–Fe powders milled for different times. The spectra were fitted by HFD as illustrated in figure 4. The starting powder
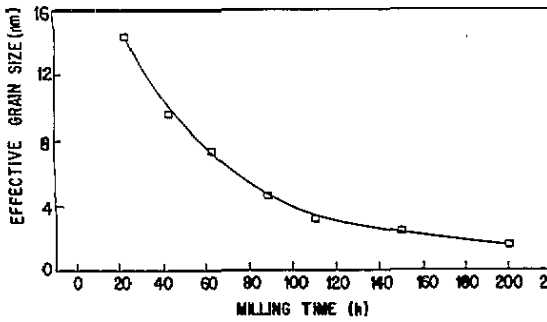
Figure 2. Effective crystallite size calculated using the Scherrer equation.

exhibits a well defined, magnetically split spectrum with a broad HFD which has an average hyperfine field of 16 T as expected for crystalline bulk samples (Kuwano and Ono 1977). After milling, an absorption line in the centre of the spectra appears corresponding to a peak centred around 2 T in the HFD curve (figure 4). The intensity of this peak increases with increasing milling time at the expense of the higher-field component which, after milling for 150 h, is below the limit of detection by Mössbauer spectroscopy. It can be seen that, although the high-field component decreases with increasing milling time, it keeps the same almost constant average B_{hf}-value as that of the starting material. This indicates that some residual crystallites remain in the samples and that these crystals have a composition similar to the starting material.
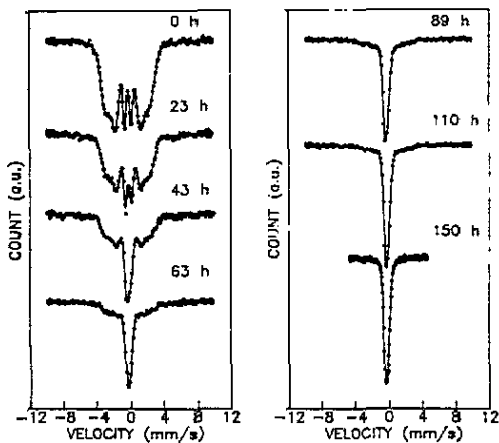

Figure 3. Mössbauer spectra measured at 4.2 K for Cr–Fe powder before and after mechanical milling for various times (a.u., arbitrary units).
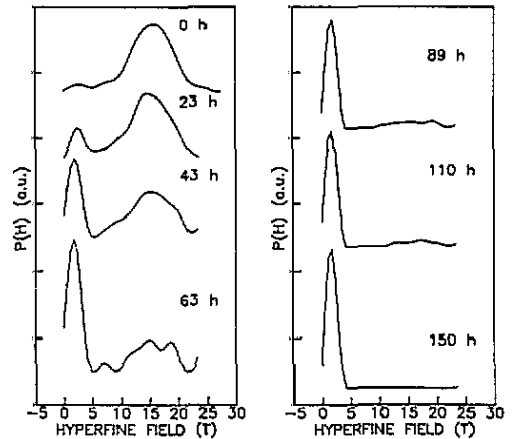
Figure 4. HFDs obtained from 4.2 K Mössbauer spectra shown in figure 3 (a.u., arbitrary units).

Figure 5 shows the Mössbauer spectra measured at RT. It can be seen that, after milling, the single line broadens and a shoulder appears after 43 h as indicated by the arrow. This shoulder becomes clearer with increasing milling time up to 110 h, when the broadening of the absorption line makes it invisible. The starting powder exhibits a paramagnetic singlet with an IS of -0.105 mm s^{-1} (all ISs are relative to α-Fe) and a linewidth W of 0.31 mm s^{-1}. To fit these broadened spectra, Kuwano et al (1992) assumed an HFD based on the fact that a saturation magnetization of about 2 emu g^{-1} was observed at RT. However,
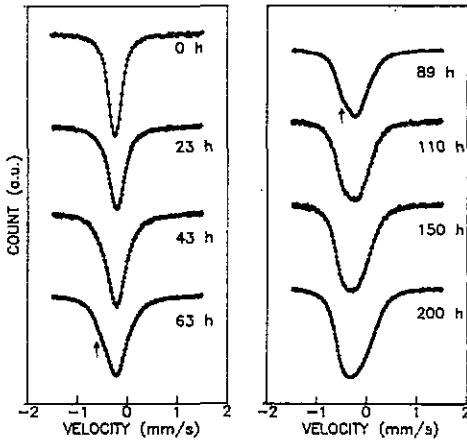
Figure 5. RT Mössbauer spectra of Cr–Fe powder before and after mechanical milling for various times (a.u., arbitrary units).
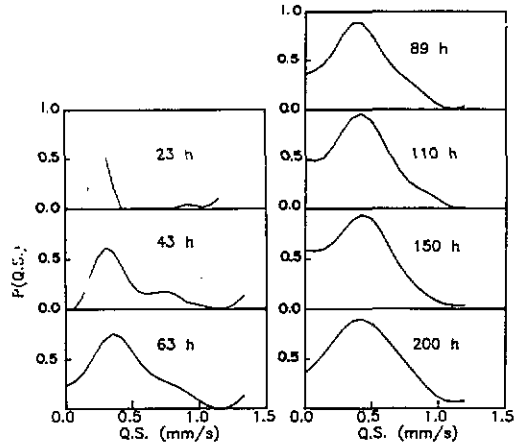
Figure 6. QSD obtained from the RT Mössbauer spectra shown in figure 5.

it must be noted that such a small saturation magnetization can be induced by a very small amount of impurities from magnetic materials with high saturation magnetizations. On the other hand, in such a material with a disordered structure, one can expect that a distribution of quadrupole interactions plays an important role. Furthermore, we performed recently a 'temperature dependence' Mössbauer measurement from RT to 400 °C on sample FC200 (to eliminate the effect of structural relaxation on heating, as we shall discuss below, the sample was annealed just below the crystallization temperature). If the spectra were fitted by a QSD, the average QS value follows a $T^{3/2}$ law which is seen in the T-dependence of electric field gradient for many materials with non-cubic structures (Mahnke *et al* 1979). This behaviour supports the view that the broadening of the RT spectra is mainly due to the distribution of quadrupole interactions.

Therefore, a QSD is assumed here (figure 6) to fit the RT spectra overlapped with a singlet resulting from the residual crystalline component (mentioned above) with an IS$= -0.105$ mm s^{-1} and $W = 0.35$ mm s^{-1}. It can be seen from figure 6, for short milling times, that the QSD shows a narrow peak centred at about 0.25 mm s^{-1}. As the milling time increases, this peak broadens and shifts to high QS values. This indicates that the ball milling increases both the asymmetry and the distribution of the atomic configurations, i.e. leads to structural disorder. Figure 7 shows the milling time dependences of the average IS ($\overline{\text{IS}}$) of the QSD component and the residual crystalline component (broken line). The $\overline{\text{IS}}$ corresponding to the QSD component is more negative than that of the crystalline component, indicating a higher s-electron density at Fe nuclei. This may be induced if the QSD component corresponds to a structure which has a more densely packed nature than the original BCC structure. In such a structure the Fe nuclei could obtain more s electrons from the Cr atoms whose electronegativity is lower than that of the Fe atoms (Sumiyama *et al* 1987). Clearly, owing to the more negative $\overline{\text{IS}}$, the shoulder shown in figure 5 is attributed to the densely packed component. It can also be seen that, for milling times above 43 h, a tail appears in the QSD curve (figure 6) with a higher QS value and also a higher $\overline{\text{IS}}$ of about 0.08 mm s^{-1}, which is somewhat larger than that of the BCC phase. Using the above information on IS, this component may be attributed to loosely packed atomic configurations

which may also be responsible for the increase in the average IS for milling times greater than 150 h (figure 7).
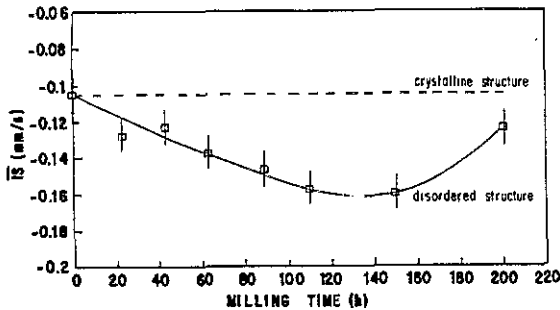

Figure 7. The milling time dependence of ISs, relative to α-Fe, of the disordered structural component and the residual crystalline component.

3.3. Differential scanning calorimetry

Figure 8 shows the DSC curve for the powder sample FC200. The figure exhibits two exothermic peaks with onset temperatures at about 662 and 799 K. The intensity of the peak at 662 K is much smaller than that at 799 K. The exothermic energies for the peaks at 662 K and 799 K are 5.75 J g^{-1} and 27.72 J g^{-1}, respectively.

A powder sample FC200 was heated in vacuum at the same rate as that of the DSC from RT to 753 K (a temperature between the two exothermic peaks of the DSC curve) and then quenched in water. The x-ray diffraction pattern of this sample shows that the diffracted maximum increases and the linewidth becomes narrower. No second metastable phase was observed. An additional characterization of the same powder was obtained from the RT Mössbauer spectrum and the corresponding QSD in figure 9, curve (b). For comparison, the Mössbauer spectrum as well as the QSD for the as-prepared sample FC200 are shown in figure 9, curve (a). It can be seen that, on heating the sample to 753 K, the Mössbauer absorption line becomes narrow and the lower QS components increase at the expense of the higher QS components (corresponding to the tail) in the QSD curve for the as-prepared sample FC200. This may be interpreted as being due to the occurrence of structural relaxation and may be responsible for the low-temperature exothermic peak as a similar behaviour occurs in Si amorphous films (Avillez *et al* 1989). Figure 9, curve (c) shows the RT Mössbauer spectrum of the powder sample FC200 annealed at 873 K for 2 h and the HFD curve (the corresponding x-ray diffraction pattern is shown in figure 1, labelled 'after crystallization'. It is seen that, when the powder is heated at temperatures above that of the second exothermic peak, a magnetically split spectrum of crystalline alloy with T_c above RT appears. Therefore, it is clear that the second exothermic peak results from the crystallization of the material.

It should be mentioned that the hyperfine field at RT for the recrystallized powder is about 22 T, which is larger than that of the starting sample (16 T) measured at 4.2 K. As mentioned above, crystallization leads to a precipitation of Cr-rich phase, so that the remaining part of the alloy has a higher Fe content. Therefore, it is understandable that the larger hyperfine field for the recrystallized sample is due to the Fe-rich Cr–Fe alloy. The Cr-rich phase which exhibits a paramagnetic behaviour leads to an absorption peak in the centre of the spectrum.
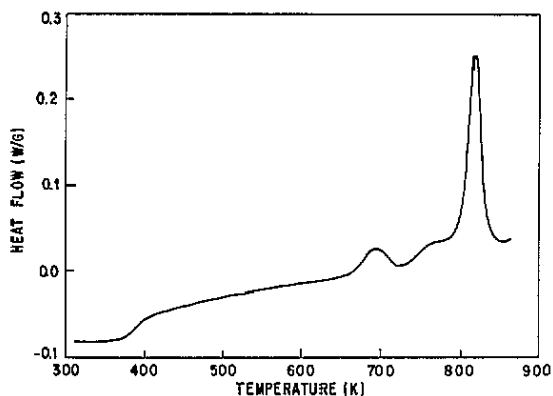
Figure 8. The DSC plot at 20 K min^{-1} for Cr–Fe powder milled for 200 h.

4. Discussion

The results of the Mössbauer measurements indicate that mechanically milled Cr–Fe powders are composed of a residual crystalline component and a structurally disordered component. Figure 10 shows the milling time dependences of the fractions for both components. The residual crystalline component remains a singlet at RT and splits into magnetic spectra at 4.2 K with a hyperfine field similar to that of the initial alloy. The intensity of this component decreases with increasing milling time. After 150 h, although defined by RT Mössbauer spectra, it cannot be detected at 4.2 K since the absorption area is spread out in a magnetic distribution spectrum. The relative areas of this component obtained from both RT and 4.2 K Mössbauer spectra are plotted in figure 10 and good agreement is obtained.
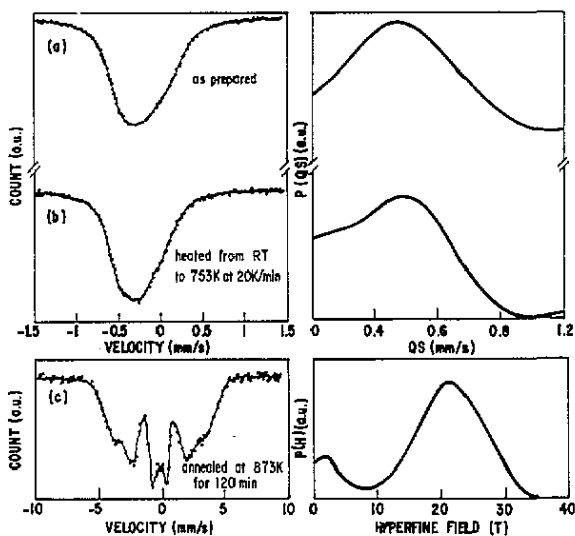

Figure 9. RT Mössbauer spectra and the corresponding fits of the powder sample FC200 (a.u., arbitrary units): curve (a), as prepared; curve (b), heated from RT to 753 K at a rate of 20 K min^{-1}; curve (c), annealed at 873 K for 2 h.

The disordered component is attributed to two disordered structures: random densely packed and random loosely packed atomic configurations; these are characterized by the
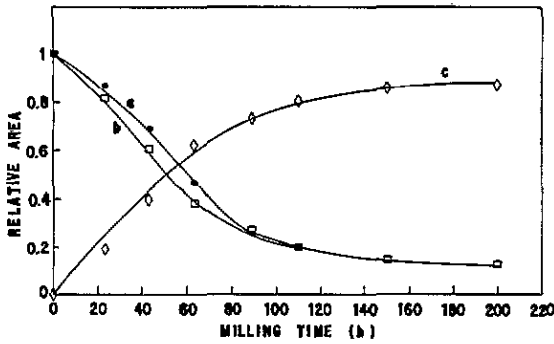
Figure 10. The fractions of the components of mechanically milled Cr–Fe powder: ●, residual crystalline component obtained from 4.2 K Mössbauer spectra; □, crystalline component obtained from RT Mössbauer spectra; ◊, the disordered structural component.

peak and the tail, respectively, on the QSD curve (figure 6). Since the $\overline{\text{IS}}$ of both disordered structures are different, the milling time dependence of the $\overline{\text{IS}}$ (figure 4) may be explained as follows. Below 110 h, the formation of the random densely packed structural component dominates the amorphization process while, above 150 h, the contribution of the loosely packed component becomes important.

The amorphization of Cr–Fe alloy through MM may be attributed to the combination of two factors. One is the accumulation of lattice defects which leads to an increase in structural disorder. Such a process may be associated with the continuous changes in QSD (in figure 6) and IS (in figure 7). However, the increase in the density of the lattice defects does not occur to the same extent for every metal. In a recent study, it was found that, during the MM of pure Fe powder, the density of lattice defects may reach a saturation value with an ordering correlation length of about 6.5 nm. On the other hand, for Cr–Fe alloy, this correlation length can reach about 1.5 nm, as shown in figure 2.

The second factor to be considered concerns the stability of the σ-phase in the Cr–Fe system. According to the phase diagram, below 800 K, $Cr_{1-x}Fe_x$ alloys (Hansen 1958) may form a σ-phase in the range $0.50 < x < 0.56$. Outside this range, there is a two-phase $(\alpha + \sigma)$ region which extends from $x = 0.29$ to 0.74. In a more recent work, Kubaschewski (1982) suggested that the σ-phase is not an equilibrium phase since, after a long thermal treatment below 730 K, a homogeneous Cr–Fe alloy with a composition in the $(\alpha + \sigma)$-phase range will transform to $\alpha + \alpha_1$ (mixture of BCC Fe-rich and BCC Cr-rich phases). However, even if the σ-phase is metastable, the stability is very high and, once formed, it is difficult to transform it to the equilibrium phases (Dubiel and Inden 1987). Since the σ-phase has a topologically densely packed structure, it may be acceptable that a metastable random densely packed structure can be formed in the Fe concentration range $0.29 < x < 0.74$ where the σ-phase appears. In a recent study, in which $Cr_{1-x}Fe_x$ films were prepared by thermal evaporation, amorphous alloy films were obtained in this Fe concentration range while, outside this range, a BCC structure appeared (Xia et al 1993). Since, in the present study, MM leads to an increase in the Fe concentration, the composition of the milled sample eventually enters the $(\sigma + \alpha)$ region. At the same time, the increase in defect density may lead to structural relaxation with a corresponding increase in atomic density. In other words, the accumulation of lattice defects favours the formation of a metastable random densely packed structure. As a consequence, an extremely defective structure may be finally obtained and the defect spacings can reach atomic dimensions. Such a structure, according to Hornbogen (1979), can be assumed to be amorphous. The smaller crystallization enthalpy for the present sample, 27.72 J g^{-1}, compared with those for the usual metal glasses may be associated with a smaller phase transformation enthalpy from a densely packed structure

to the BCC structure as discussed above.

The loosely packed component may result from grain boundaries, which may be formed in the following ways. The ball milling increases the number of dislocations inside the grains by cold work. As the dislocation concentration increases, the dislocations start to cross each other and their motion is gradually impaired because of the formation of tangles, until the grains finally break up into smaller grains. Subsequently, these grains are cold welded together during the ball-milling process (Schultz 1988), producing small subgrains in the material. This process will yield a large number of grain boundaries.

According to the model proposed by Buschow and Beekmans (1980), the crystallization of an amorphous alloy takes place by atomic diffusion. The activation energy for diffusion is the energy required to form a hole of the same size as the smaller atom in the alloy. Since Fe and Cr have similar atomic sizes, the activation energy for forming a hole should be higher than that for a system composed of atoms with rather different atomic sizes. Furthermore, according to the calculation of Miedema and Niessen (1982), there is almost no volume correction for either element in Cr–Fe alloy, which implies that the negative chemical enthalpy of mixing is small. Thus the driving force for crystallization in this case comes from the enthalpy contribution due to the disorder (comparable with the heat of fusion for liquid, although smaller). In a first-order approximation, this enthalpy is related only to the melting point of each constituent of the amorphous alloy (Loeff *et al* 1988). Therefore, it is interesting to note that, despite the difficulty of obtaining amorphous alloys in the Cr–Fe system because of the similarity of their atomic sizes, once a disordered structure is formed, as in the present study by MM, it may resist crystallization and remain as a metastable structure.

In conclusion, we have found that a disordered structure can be obtained by MM in a BCC $Cr_{72}Fe_{28}$ alloy. During milling, the contamination from the tools caused the Fe concentration of the alloy to increase to 35 at.%, which is in the Fe concentration range of the $(\sigma + \alpha)$-phase field (σ has a densely packed structure) in the phase diagram. The formation of the disordered structure may be due to the accumulation of lattice defects. For the present alloy, the density of lattice defects may become extremely high and, as a consequence, an extremely defective structure (amorphous structure) is formed. The experimental results also revealed that, with increasing milling time, a grain boundary component appears. After milling for 200 h, about 10% of residual crystals seem still to remain in the material. The mechanically milled powders show a strong structural relaxation on heating to a temperature just below the crystallization temperature of 799 K as indicated by DSC measurement. The thermal stability of such a structure may be due to the difficulty of the interdiffusion in the Cr–Fe system in this temperature range.

Acknowledgments

References

Avillez R R, Clevenger L A and Thompson C V 1989 *J. Mater. Res.* **4** 1057

Birringer R, Gleiter H, Klein H P and Marquardt P 1984 *Phys. Lett.* **102A** 365

Brand R A and Le Caer G 1988 *Nucl. Instrum. Methods* B **34** 272

Buschow K H J and Beekmans N M 1980 *Solid State Commun.* **35** 233

Davies H A 1983 *Amorphous Metallic Alloys* ed F E Lubosky (London: Butterworth) p 8

Dubiel S M and Inden G 1987 *Z. Metallk.* **78** 544

Giessen B C 1982 *Proc. 4th Int. Conf. on Rapidly Quenched Metals (Sendai, 1981)* vol 1 (Sendai: Japan Institute of Metals) p 213

Hansen M 1958 *Constitution of Binary Alloys* (New York: McGraw-Hill) p 527

Hellstern E and Schultz L 1987 *Proc. 6th Inter Conf. Liquid Amorphous Metals (Garmisch-Partenkirchen 1986)* vol 2 (Munich: Oldenburg) p 215

Hornbogen E 1979 *Metall. Trans.* A **10** 949

Koch C C, Cavin O B, Mckamey C G and Scarbrough J O 1983 *Appl. Phys. Lett.* **43** 1017

Kubaschewski O 1982 *Iron Binary Phase Diagrams* (Berlin: Springer)

Kuwano H and Ono K 1977 *J. Phys. Soc. Japan* **42** 72

Kuwano H, Ouyang H and Fultz B 1992 *Mater. Sci. Forum* **88–90** 537

Loeff P I, Weeber A W and Miedema A R 1988 *J. Less-Common Met.* **140** 299

Mahnke H E, Dafni E, Rafailovich M H, Sprouse G D and Vapirev E 1979 *Phys. Lett.* **71A** 112

Miedema A R and Niessen A K 1982 *Physica* B **114** 367

Rodríguez V A P, Saitovitch E B, Xia S K, Larica C and Lima J C 1991 *Hyperfine Interact.* **69** 721

Saiki K, Saito K, Onishi K, Numata T, Inokuchi S and Sakurai Y 1985 *IEEE Trans. Magn.* **MAG-21** 1471

Schultz L 1988 *J. Less-Common Met.* **145** 233

Schwarz R B and Koch C C 1986 *Appl. Phys. Lett.* **49** 146

Sumiyama K, Ohshima N and Nakamura Y 1987 *Trans. Japan. Inst. Met.* **28** 699

Weast R C (ed) 1965–6 *Handbook of Chemistry and Physics* 46th edn (Boca Raton, FL: Chemical Rubber Company) p f-119

Weeber A W, Bakker H, Heijligers H J M and Bastin G F 1987 *Europhys. Lett* **3** 1261

Weeber A W, Van der Meer K, Bakker H, de Boer F R, Thijsse B J and Jongste J F 1986 *J. Phys. F: Met. Phys.* **16** 1897

Xia S K, Saitovitch E B and Larica C 1993 to be published